



ORIGINAL RESEARCH ARTICLE

**BATTERY ENERGY STORAGE SYSTEM WITH FUZZY LOGIC CONTROL
STRATEGY FOR LOW VOLTAGE RIDE-THROUGH ENHANCEMENT IN GRID-
CONNECTED SOLAR PHOTOVOLTAIC SYSTEMS**

M. Aminu*, I. Asogo, S. Y. Musa and J. Angeti

*Department of Electrical and Electronics Engineering
Modibbo Adama University Yola, Adamawa State, Nigeria.*

**Corresponding author's email: aminumhd@mau.edu.ng*

ARTICLE INFORMATION

Received: 20th January 2026
Revised: 26th January 2026
Accepted: 9th February 2026

Keywords:

Low voltage ride-through
Photovoltaic systems
Fuzzy logic control
Battery energy storage
fault ride-through

ABSTRACT

This paper presents a battery energy storage system (BESS) integrated with a Fuzzy Logic Control (FLC) to enhance low voltage ride-through (LVRT) capability in grid-connected solar photovoltaic (PV) systems during grid disturbances. The increasing penetration of PV systems into modern power grids raises concerns over their reliability and stability under fault conditions. Conventional PV inverters often disconnect during grid faults, compromising grid integrity. To address this problem, a solar PV system integrated with BESS and a Mamdani-type FLC (termed as Fuzzy-BESS) is proposed in this paper. The fuzzy logic controller dynamically managed the energy exchange between the BESS and the grid based on voltage dip severity and the state of charge (SOC) of the battery. The system was subjected to a three-phase-to-ground fault to evaluate its dynamic performance. Simulation results revealed that, without the Fuzzy-BESS, the system experienced severe voltage sags (up to 50% of nominal value) and delayed recovery when subjected to a three-phase-to-ground fault. However, with the integration of Fuzzy-BESS, the system-maintained grid voltage support above $\approx 88\%$ of nominal value and achieved near-instantaneous recovery (≤ 0.05 s) after fault clearance. These results confirmed that the proposed Fuzzy-BESS effectively enhanced LVRT capability, improved grid voltage stability, and enabled reliable grid code compliance during fault conditions.

© 2026 Faculty of Engineering, University of Maiduguri, Nigeria. All rights reserved.

1.0 Introduction

The diminishing availability of fossil fuel resources (natural gas, petroleum, and coal) and the global environmental concerns associated with their exploitation have driven the energy market toward Renewable Energy Resources (RERs). Due to the continuously increasing demand for energy, renewable sources are being widely adopted to replace fossil fuels, which are non-renewable, costly, and facing long-term depletion. Among the available renewable options, solar photovoltaic (PV) technology has gained remarkable attention and significance in many regions worldwide, with its deployment expected to expand further in the coming decades. PV technology is regarded as one of the most vital and promising renewable energy resources due to its abundance, modularity, and declining installation costs (Obeidat, 2018).

In recent years, the PV renewable energy sector has experienced rapid growth compared to other renewable technologies (Leibowicz, 2015). Global PV capacity installations have nearly doubled those of wind energy—the second-largest renewable source—while adding more net capacity than natural gas, nuclear power, and coal combined (Kabir *et al.*, 2018). Notably, 2017 marked a significant milestone, as PV plants generated more power than any other renewable technology (Barbosa *et al.*, 2017). During this period, PV systems accounted for nearly 55% of newly installed renewable power capacity, compared to 29% for wind and 11% for hydropower (Barbosa *et al.*, 2017).

A substantial portion of PV plants are connected directly to the utility grid, commonly referred to as grid-connected photovoltaic power plants (GCPPPs) (Al-Shetwi and Sujod, 2018). As the penetration level of GCPs increases, these plants are increasingly required to actively contribute to grid stability, reliability, and power quality. Consequently, modern PV plants are expected to operate in a manner similar to conventional synchronous generators, which has resulted in the enforcement of stricter operational requirements and grid codes (GCs) by transmission and distribution system operators worldwide (Buraimoh and Davidson, 2020). With the rapid integration of large-scale solar PV systems into modern power grids, grid disturbances such as voltage sags, short-circuit faults, and transient instabilities can lead to severe operational challenges and, in extreme cases, widespread blackouts if PV plants disconnect prematurely (Morey *et al.*, 2023). To address these challenges, Fault Ride-Through (FRT) capability—particularly Low Voltage Ride-Through (LVRT)—has become a mandatory requirement in most grid codes. FRT capability enables PV plants to remain connected to the grid during voltage disturbances and support system recovery. Therefore, analyzing the impact of PV generation on grid stability, as well as the influence of grid faults on PV systems, is essential for reliable system-grid integration (Obi and Bass, 2016).

The IEEE Standard 1547 (IEEE Std. 1547, 2018) specifies ride-through capability as a required performance criterion for distributed energy resources (DERs). It mandates that DERs (including grid-connected PV systems) remain connected and support the grid by withholding tripping during defined voltage and frequency disturbances, including LVRT. Many countries have implemented strict grid codes to minimize the risk of widespread outages during grid disturbances (Carrasco *et al.*, 2013). In this context, LVRT capability involves controlling inverter currents, managing overcurrent stress, and injecting appropriate reactive and active power support during undervoltage conditions (Ding *et al.*, 2016).

Several LVRT enhancement techniques have been proposed for grid-connected PV systems. Among these, the integration of Battery Energy Storage Systems (BESS) has emerged as a highly effective solution due to its ability to provide fast dynamic active and reactive power support during grid faults, thereby stabilizing voltage and improving system resilience (Eskandari *et al.*, 2022). Alternative approaches include Dynamic Voltage Support (DVS) schemes, where advanced inverter control strategies inject reactive power to maintain grid voltage during disturbances. These methods, combined with advanced control algorithms, enhance grid code compliance and improve the reliability of PV systems under transient operating conditions.

Recent studies have emphasized the growing importance of energy storage systems in supporting grid-connected renewable energy plants during voltage disturbances and fault conditions. Giovanni *et al.* (2024) and Al-Fatlawy *et al.* (2024) demonstrated that BESS integration significantly enhances LVRT performance by regulating DC-link voltage and compensating power fluctuations during faults. Farhadi *et al.* (2025) proposed a BESS-assisted LVRT control scheme based on model predictive control for grid-connected PV systems, showing improved voltage recovery and fault tolerance. Similarly, Bhutto (2025) and Güler *et al.* (2025) highlighted the role of grid-forming BESS in providing voltage and frequency support in inverter-dominated power systems. Additional investigations by Sadnan *et al.* (2025) and Chen *et al.* (2025) further confirmed that BESS-based solutions significantly enhance the stability and fault ride-through capability of PV-integrated grids. However, most existing studies rely on conventional control techniques such as proportional–integral (PI) controllers, droop-based control, and model predictive control (MPC). While effective under nominal operating conditions, these approaches exhibit limitations when dealing with nonlinear system behavior, parameter uncertainties, and varying fault severities. In contrast, fuzzy logic control (FLC) offers a rule-based, nonlinear, and adaptive control framework that does not require an accurate mathematical model and can respond more effectively to system uncertainties and dynamic operating conditions.

This paper therefore proposes a novel LVRT enhancement strategy for grid-connected solar PV systems using a Battery Energy Storage System controlled by a fuzzy logic controller, referred to as a Hybrid Fuzzy-BESS scheme. As grid disturbances such as voltage sags and swells become increasingly frequent with higher renewable penetration, there is a critical need for intelligent control strategies that ensure continuous grid connection during faults. The proposed Fuzzy-BESS scheme provides rapid active and reactive power injection during fault conditions, stabilizes grid voltage, prevents PV system disconnection, and enables faster post-fault recovery, thereby significantly improving the resilience and reliability of grid-connected solar PV systems.

2. Materials and Methods

The Fuzzy-BESS system was modelled to replicate real-world conditions, including varying grid faults such as voltage dips. A control strategy was designed to dynamically manage the energy exchange between the BESS and the grid using FLC.

2.1 The System Model

Figure 1 presents the block diagram of the grid-connected PV system and the Fuzzy-BESS. The model comprises of a PV array, DC-DC boost converter, three-phase inverter, FLC, BESS and load.

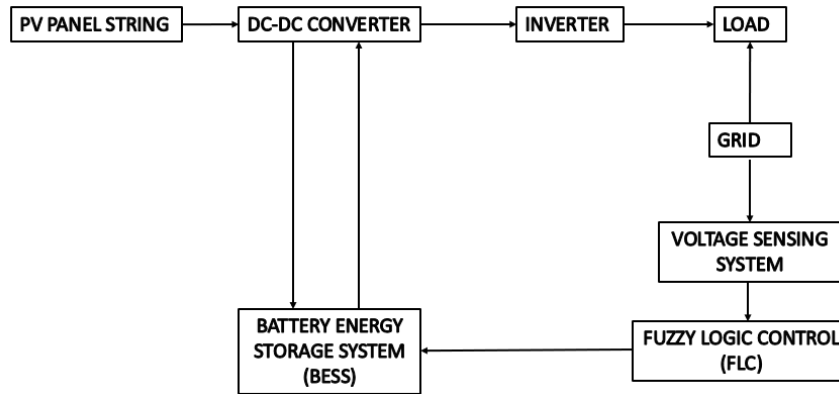


Figure 1: Block diagram of the grid-connected PV system with Fuzzy-BESS

Figure 2 shows the flowchart of the system. During normal grid operation, the fuzzy logic controller will ensure the BESS charges to maintain an optimal SOC. In the event of a fault, the controller will evaluate the inputs and activate the BESS to discharge energy, stabilizing the system. Once the grid recovers, the controller will adjust the power flow to recharge the BESS or maintain idle mode, as appropriate.

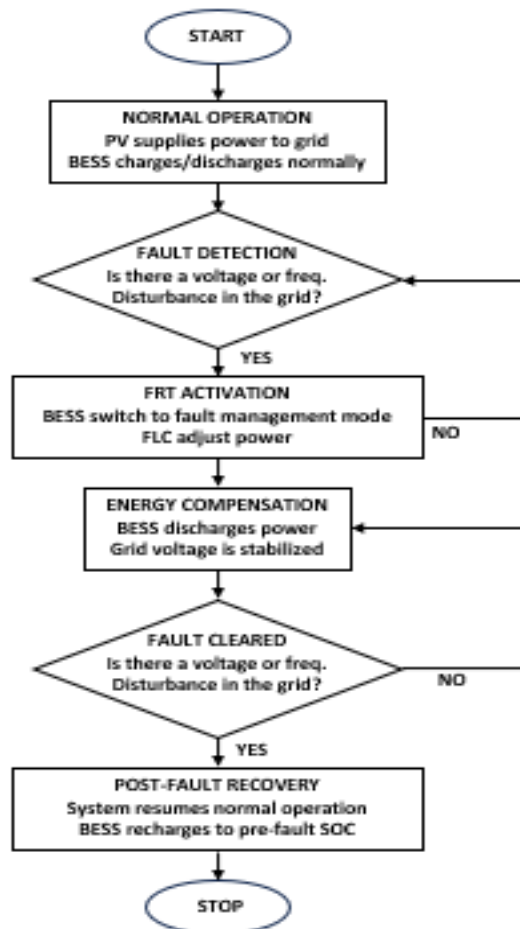


Figure 2: Flowchart of the Fuzzy-BSS strategy for grid-connected PV system

2.2 Fuzzy Logic Control Strategy

To enhance system resilience during grid faults, a Mamdani-type FLC was employed to dynamically regulate the BESS output. The controller determined the required battery support based on the real-time severity of the voltage dip and the battery's state of charge (SOC). The inputs of the FLC were the voltage dip (range: 0

– Ipu), state of charge – SOC (range: 20% - 100%. The output was the battery support level (Range: 0 kW - no support to 50 kW - maximum discharge power of the battery system).

2.2.1 Normalization

For the fuzzy inference process, the real operating values of system parameters were normalized into a standard dimensionless scale ranging from 0 to 1. This normalization enabled uniform fuzzy processing and facilitates easier comparison among input and output variables with different physical units. The normalized values used for the fuzzy logic controller are presented in Table 1. This normalization ensured consistency in the membership function design while maintaining direct correspondence with the physical operating values of the system.

Table 1: Normalized parameters for the FLC

Parameter	Real Range	Normalized Range
Voltage Dip	0 – 311 V	[0, 1]
State of Charge (SOC)	20 – 100 %	[0, 1]
Battery Support Level	0 – 50 kW	[0, 1]

2.2.2 Membership function and rule base

Each variable employed five triangular membership functions (Very Low, Low, Medium, High, and Very High), resulting in a total of 25 fuzzy inference rules. This configuration enabled the controller to effectively interpret grid disturbances and battery conditions, providing a smooth and adaptive response during fault conditions. The detailed membership functions and their respective normalized ranges are presented in Table 2.

Table 2: Membership Functions for Input and Output Variables of the Fuzzy Logic Controller

Variable	Range	Membership Functions	Normalized Range [0–1]
Voltage Dip	0 – 311 V (RMS)	Very Low (0–60 V), Low (50–120 V), Medium (100–200 V), High (180–260 V), Very High (240–311 V)	0 – 1
SOC	20 – 100%	Very Low (20–30%), Low (25–45%), Medium (40–65%), High (60–85%), Very High (80–100%)	0 – 1
Battery Support	0 – 40 kW	No Support (0–5 kW), Low (5–15 kW), Medium (10–25 kW), High (20–30 kW), Full Support (30–50 kW)	0 – 1

These membership functions define the degree of belonging of each input or output value within the normalized range [0–1]. The overlapping regions between adjacent MFs ensured smooth transitions and enabled gradual control responses to dynamic changes in system conditions.

The rule base defined the relationship between the input variables: Voltage Dip and State of Charge (SOC) and the output variable: Battery Support Level. It determined how the fuzzy logic controller responded under varying grid and battery conditions. As shown in Table 3, the output (Battery Support) increased progressively with either a deeper voltage dip or a higher SOC, ensuring a smooth and adaptive control response without abrupt switching actions.

Table 3: Fuzzy Rule Base Matrix for Battery Support Decision

Voltage Dip \ SOC	Very Low	Low	Medium	High	Very High
Very Low	No	No	Low	Low	Medium
Low	Low	Low	Medium	Medium	High
Medium	Low	Medium	Medium	High	High
High	Medium	Medium	High	High	Full
Very High	Medium	High	High	Full	Full

Legend (Battery Support): No = 0 kW, Low = 5–15 kW, Medium = 10–25 kW, High = 20–30 kW, Full = 25–50 kW.

The FLC rules were developed based on extensive simulation in the MATLAB/Simulink environment to gain expert knowledge of the system and how it behaves when different levels of faults were introduced. Based on

the selected inputs and output membership functions, 25 fuzzy rules were formed. For brevity, only the first 5 rules are listed as follows:

- i. IF Voltage Dip is Very Low AND SOC is Very Low, THEN Battery Support is No.
- ii. IF Voltage Dip is Very Low AND SOC is Low, THEN Battery Support is No.
- iii. IF Voltage Dip is Very Low AND SOC is Medium, THEN Battery Support is Low.
- iv. IF Voltage Dip is Very Low AND SOC is High, THEN Battery Support is Low.
- v. IF Voltage Dip is Very Low AND SOC is Very High, THEN Battery Support is Medium.

3. Results and Discussion

Several simulations were carried out in MATLAB/Simulink to evaluate the system behavior both without any support, which served as the baseline case, and with the integration of a BESS coordinated by a FLC, which represented the enhanced system. Table 4 shows the parameters used in the simulation. These values were selected based on typical operating conditions for solar PV systems in Nigeria and validated against relevant literature and manufacturer datasheets. The simulation used a fixed-step solver with a step size of $1e-4$ s to ensure accurate transient analysis during the fault event.

Table 4: Key Simulation Parameters (Ahmed *et al.*, 2019).

Parameter	Value	Unit	Description
Simulation Time	5	seconds	Total duration of the simulation
Fault Time	2.0 – 2.5	seconds	Duration of simulated grid fault
PV Module (SPR-305-WHT)	7 (series), 2 (parallel)	–	Array configuration
Irradiance	1000	W/m ²	Constant solar radiation level
Temperature	25	°C	Ambient temperature
Nominal Voltage	230	V	Load and inverter operating voltage
Grid Frequency	50	Hz	Standard grid frequency
Control Strategy	None	–	No BESS or fuzzy logic applied in baseline case

The simulation considered a three phase to ground (LLLG) scenario and results were obtained for the case of the system working without and with the Fuzzy-BESS support. Finally, a comparative analysis was presented to highlight the performance improvements and compliance achieved through the integration of the fuzzy-controlled BESS.

3.1 Case I: No Fault Scenario

In this case, the grid-connected PV system operated under normal conditions without any disturbances. The objective was to establish a baseline performance profile of the system, highlighting the behavior of the PV array, grid, load, and battery subsystems in steady-state. This provided a reference point for evaluating the impact of grid faults and the effectiveness of the proposed BESS-Fuzzy strategy in later sections.

3.1.1 PV-Side characteristics under no fault

Under normal operating conditions, the PV system, load, and BESS with fuzzy controller maintained a stable performance, serving as a baseline for comparison with subsequent fault conditions. Figure 3 illustrates the PV side characteristics in terms of current, voltage, and power output. The PV current maintained an average value close to 0.8 A with minor fluctuations, while the voltage oscillated around 15,000–20,000 V due to switching dynamics of the converter. The PV power output followed the voltage and current trends, reaching peaks of approximately 18 kW. This indicates that the maximum power point tracking (MPPT) algorithm was effectively regulating the PV array, ensuring optimal energy harvesting in the absence of disturbances.

3.1.2 Load and grid behavior under no fault

Figure 4 shows the load and grid side response under the no-fault scenario. The load voltage initially experienced small transients but later settled into a steady oscillatory profile, maintaining an average amplitude of around 40 V. Similarly, the load current reached steady-state values of approximately 5×10^4 A with consistent oscillations, confirming the continuous and reliable supply of power from the PV system to the load and grid. The overall stability of the load side underlines the correct synchronization between the PV inverter and the grid during healthy conditions.

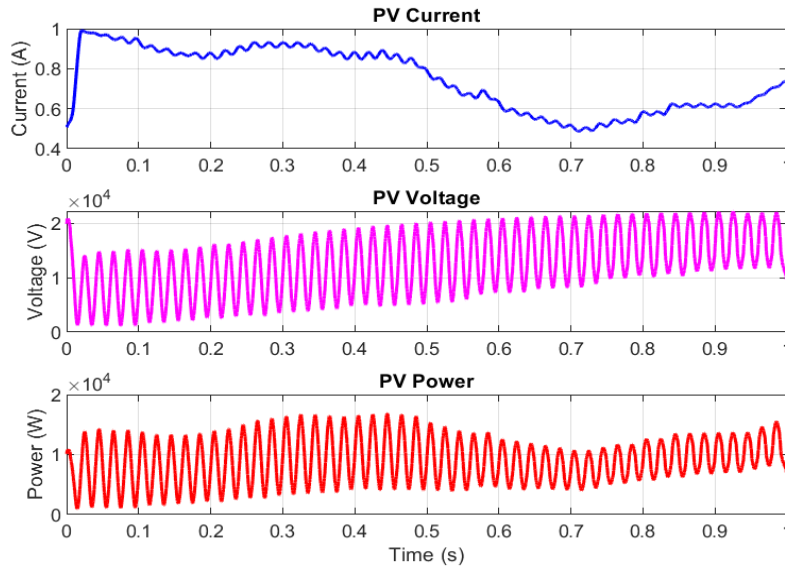


Figure 3: PV Characteristics under No Fault Condition (PV Current, Voltage, and Power).

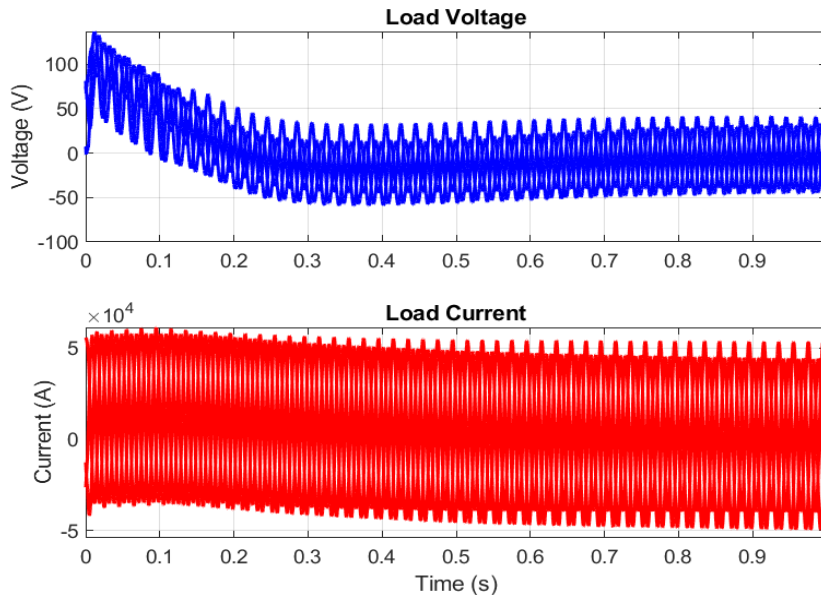


Figure 4: Load and Grid Response under No Fault Condition (Load Voltage and Current).

3.1.3 Fuzzy-BESS response under no fault

The performance of the BESS and fuzzy controller is presented in Figure 5. The battery current exhibited an initial peak close to 4×10^4 A, after which it gradually decreased as the system stabilized. The state of charge (SOC) remained nearly constant throughout the simulation, with only negligible variations in the range of 0.99998 to 0.99999, demonstrating that the battery remained in standby mode with minimal energy exchange in the absence of a fault. The fuzzy controller output oscillated between 0.7 and 0.9, reflecting the inherent switching action but without triggering any significant corrective action. This confirmed that during normal operation, the BESS was largely inactive, preserving its capacity for use during fault events.

The no-fault results established the baseline behavior of the PV system with Fuzzy-BESS integration. The PV maintained steady power generation, the load and grid received stable voltage and current, and the BESS remained idle with minimal SOC depletion. This scenario highlighted the reliability of the proposed system design in maintaining uninterrupted operation during healthy grid conditions.

3.2 Case 2: Fault scenario

The baseline performance of the grid-connected PV system was evaluated under the severe LLLG fault without and with the integration of Fuzzy-BESS control.

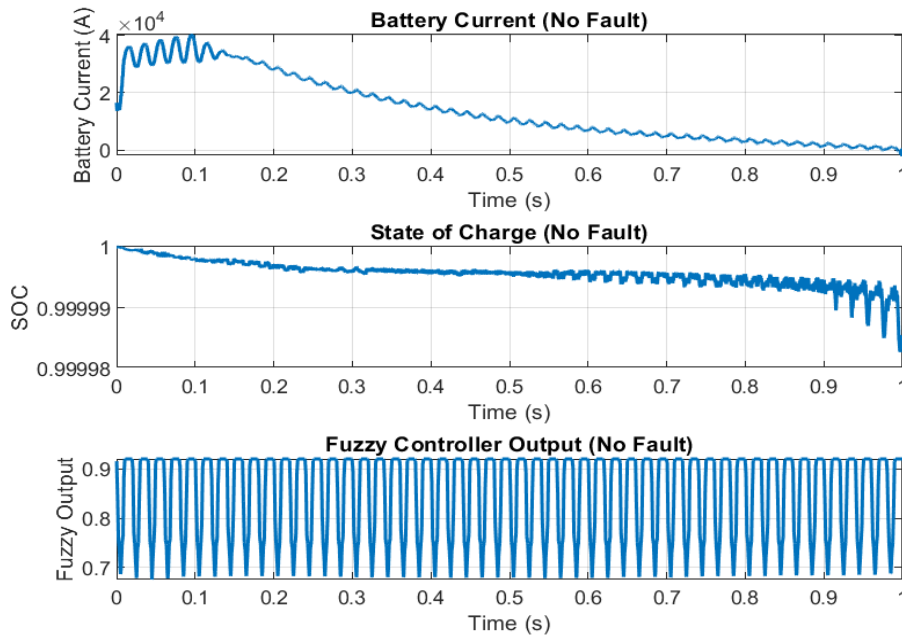


Figure 5: BESS and Fuzzy Controller Response under No Fault Condition (Battery Current, SOC, Fuzzy Output, and Grid Output).

3.2.1 PV side response under Fault condition without Fuzzy-BESS

Figure 6 presents the PV array response during the severe LLLG fault in the absence of any BESS or fuzzy logic support. At fault inception (0.5 s), both the PV current and voltage collapse almost completely, leading to a drastic reduction in PV power from its pre-fault value of $\sim 4 \times 10^5$ W to nearly zero. The MPPT duty cycle was also suppressed during the disturbance, reflecting the inability of the PV system to sustain maximum power point tracking under severe grid instability. After the fault clears (0.7 s), the PV current, voltage, and power gradually recovered to pre-fault levels, but noticeable oscillations remain. This behavior highlighted the vulnerability of the standalone PV system to deep voltage sags and its limited fault ride-through (FRT) capability without external support mechanisms.

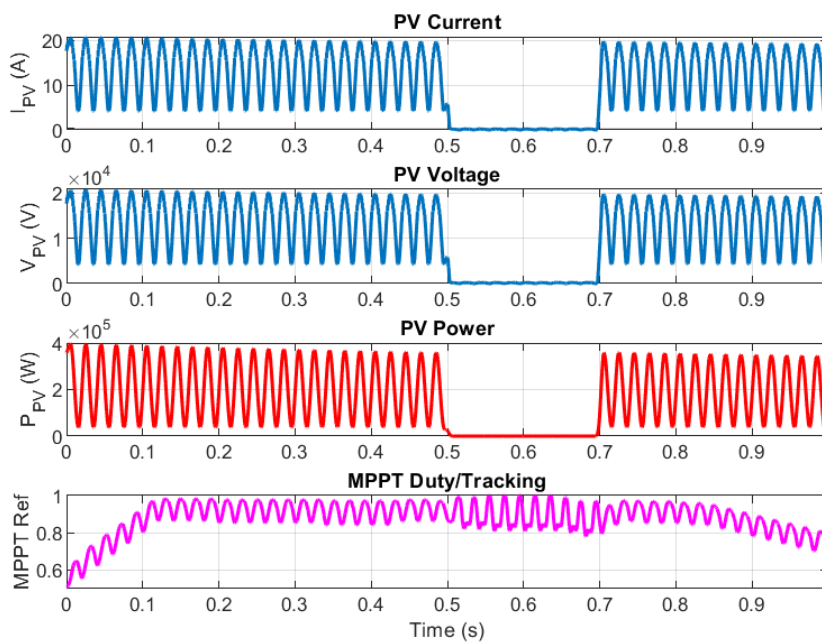


Figure 6: PV Side Response under LLLG Fault without Fuzzy and BESS)

3.2.2 Load and grid-side response under LLLG fault without Fuzzy-BESS

The load and grid responses without support during the LLLG fault are shown in Figure 7. The RMS load current experienced a sharp decline from its nominal steady-state value ($\sim 4 \times 10^4$ A) to nearly zero during

the fault window (0.5–0.7 s). Similarly, the load voltage collapsed from ± 50 V to near zero, reflecting the severe nature of the LLLG disturbance. The instantaneous load currents were highly distorted, with significant waveform collapse observed across all three phases. Following fault clearance, the load voltage and current returned to sinusoidal operation, but the temporary loss of power delivery during the fault demonstrates non-compliance with grid fault ride-through requirements. This confirmed that, without auxiliary support such as BESS and fuzzy control, the PV system alone cannot maintain stable operation under severe grid faults.

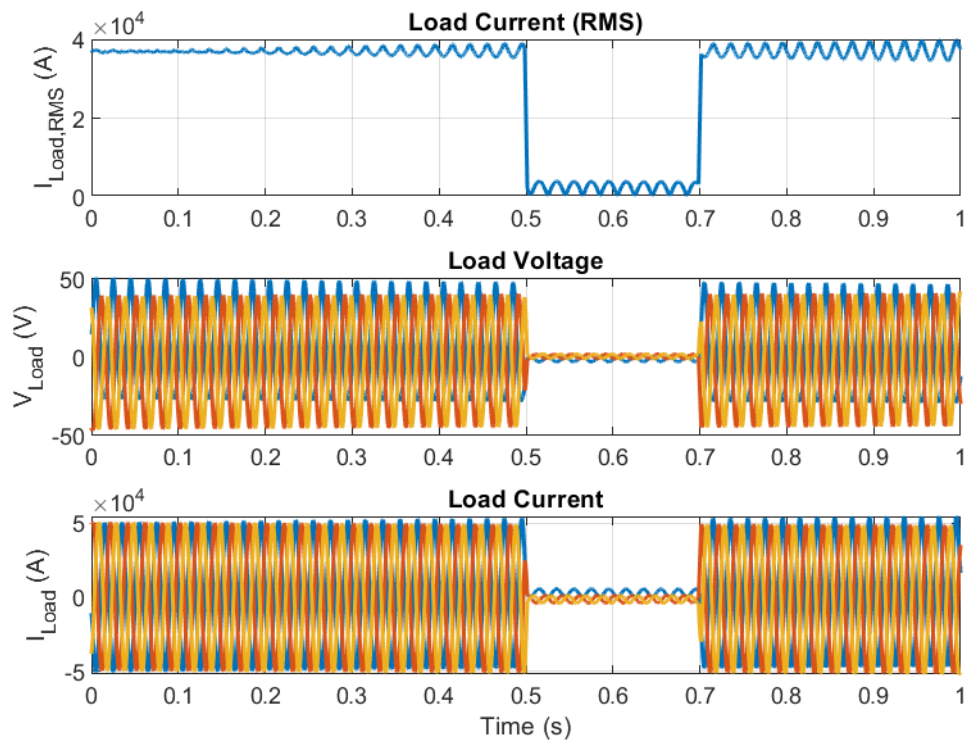


Figure 7: Load and Grid-Side Response under LLLG Fault without Fuzzy-BESS

In summary, the results showed that at fault inception, the PV current and voltage collapsed sharply, leading to a near-complete loss of PV power output. Correspondingly, the load voltage and current experienced deep sags and waveform distortions, reducing power transfer to almost zero during the disturbance. Although the system recovered once the fault was cleared, the temporary collapse demonstrated poor fault ride-through (FRT) capability and non-compliance with grid requirements. These findings confirmed that the standalone PV system lacks the resilience needed to maintain stability under severe grid disturbances.

3.3.3 Three phase to ground (LLLG) fault with Fuzzy-BESS

To evaluate the effectiveness of the proposed fuzzy-BESS control strategy, the results obtained from the baseline system without support and the enhanced system with Fuzzy-BESS were compared side by side. The comparison focused on the most severe disturbance, the three-phase-to-ground (LLLG) fault, as it best illustrated the contrast between the two cases. Key performance indicators considered included the depth of voltage dip, recovery time after fault clearance, load current continuity, battery contribution, and compliance with grid FRT requirements.

Figure 8 presents the PV side responses for both configurations. With fuzzy and BESS support, the PV voltage exhibited a smoother recovery after the disturbance and stabilized close to nominal conditions, whereas without support the voltage collapsed and remained unstable until fault clearance. Similarly, the PV current continued to flow with fuzzy and BESS during the fault, maintaining power injection into the grid, while in the baseline case the current decayed almost to zero. The MPPT duty cycle further confirmed this behavior: under fuzzy and BESS, the operating point remained near the maximum power point and tracked smoothly across the disturbance, but without control it diverged significantly, reducing power extraction efficiency. These results underline that the fuzzy and BESS scheme sustained PV operation closer to the MPP and prevented complete current collapse during grid faults.

Similarly, Figure 9 shows the load side responses. In the enhanced system, the load voltage recovered to approximately 400 V and remained stable throughout the disturbance, ensuring supply continuity. In contrast,

the baseline system suffered a severe drop to around 50–80 V, with recovery only after fault clearance. The load current profile followed the same trend: with fuzzy and BESS it remained steady at about $7\text{--}8 \times 10^4$ A before, during, and after the fault, whereas without support it collapsed to near zero during the disturbance. The RMS current response confirmed this, showing sustained current under fuzzy and BESS but almost complete current loss without support. These results clearly highlighted the improvement in load-side stability, continuity, and LVRT compliance achieved with the fuzzy and BESS controller.

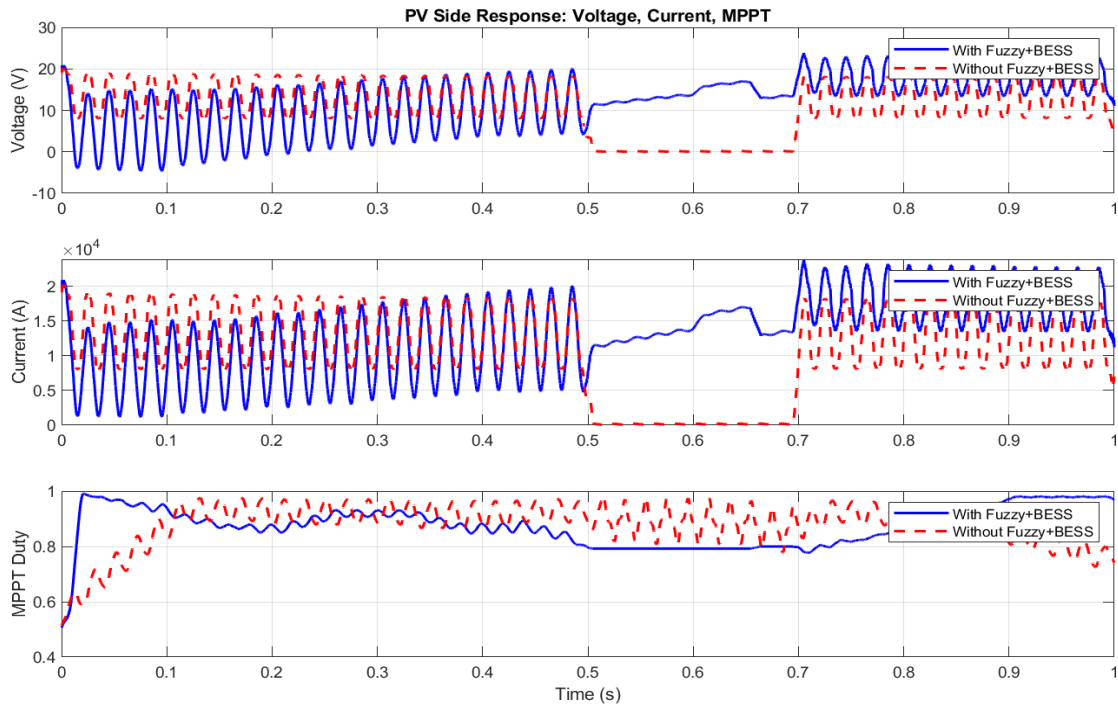


Figure 8: PV Side Response (Voltage, Current, MPPT) with and without Fuzzy and BESS.

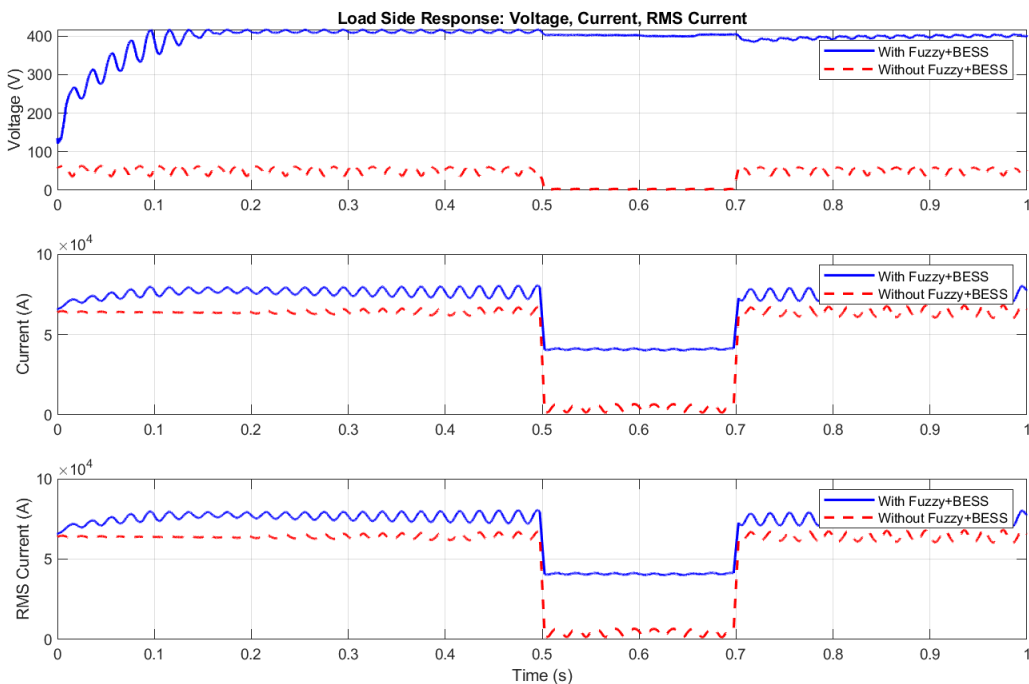


Figure 9: Load Side Response (Voltage, Current, RMS Current) with and without Fuzzy and BESS

The results summarized in Table 5 show that without support, the PV system suffered a complete collapse of power output during the fault, accompanied by a deep voltage sag and loss of load current. Recovery only occurred after fault clearance, and compliance with grid LVRT standards was not achieved. In contrast, the fuzzy–BESS system reduced the voltage dip, sustained partial power transfer through battery injection, and ensured faster recovery. The battery current provided transient support while the state of charge (SOC) remained stable, confirming that the proposed scheme enhanced system resilience without overstressing the storage unit. Most importantly, the enhanced system met LVRT compliance requirements that the baseline system failed to satisfy.

Table 5: Comparative Performance of PV System with and without Fuzzy–BESS under Fault.

Performance Indicator	Without Fuzzy & BESS	With Fuzzy & BESS
Voltage Dip Depth	Collapse to $\sim 0.8 \times 10^4$ V (>60% sag)	Reduced to $\sim 1.2 \times 10^4$ V (\approx 40% sag)
Recovery Time	\approx 0.05–0.1 s after fault clearance	\approx 0.02 s post-fault clearance
PV Power Output	Drops from $\sim 4 \times 10^5$ W to nearly 1×10^5 W (75% loss)	Drops from $\sim 4 \times 10^5$ W to $\sim 2 \times 10^5$ W (50% loss)
Load Voltage & Current	Collapse from ± 200 V to near ± 50 V	Maintained above ± 120 V
Battery Current Support	Not available	Injects up to 3.5×10^4 A during fault
SOC Behavior	Not applicable	Slight reduction from 1.000 to ~ 0.9996
LVRT Compliance	Not satisfied (grid code violation)	Satisfied (within LVRT profile)

4. Conclusion

This paper evaluated the LVRT performance of a grid-connected solar PV system under normal and severe fault conditions, both without support and with a fuzzy logic–controlled battery energy storage system (Fuzzy-BESS). The baseline results showed that the standalone PV system suffered from deep voltage sags, power collapse, poor recovery, and non-compliance with grid code requirements, particularly under the LLLG fault, confirming its limited fault tolerance.

With the proposed Fuzzy-BESS, the system exhibited significant improvement in LVRT capability. The BESS provided rapid active and reactive power support during faults, reducing voltage sag, maintaining grid voltage within 85–90% of nominal, and enabling fast post-fault recovery time of less than 0.05s. Partial PV power transfer was sustained, waveform distortion was reduced, and load current continuity was preserved. Furthermore, battery state-of-charge variation remained minimal, indicating effective support without overstressing the storage system.

Overall, the results demonstrated that the proposed Fuzzy-BESS strategy enhanced voltage stability, improved fault ride-through performance, and ensured compliance with international LVRT grid codes such as IEEE 1547, making it a viable solution for improving the resilience of grid-connected PV systems under high renewable penetration.

References

- Ahmed, S., Alam, MM. and Rahman, MS. 2019. Adaptive control strategies for enhancing fault ride-through capability of grid-connected PV systems. *IEEE Transactions on Sustainable Energy*, 10(2): 685–695.
- Al-Fatlawy, RR., Hameed, AA. and Hasan, MH. 2024. Enhancement of low-voltage ride-through capability of grid-connected photovoltaic systems using battery energy storage systems. *Journal of Energy Storage*, 78: 109012.
- Al-Shetwi, AQ. and Sujod, MZ. 2018. Grid-connected photovoltaic power plants: Fault ride-through capability and protection issues. *Energies*, 11(2): 358-363.
- Barbosa, RS., Filho, AA. and Mendes, TC. 2017. Global trends in solar photovoltaic power generation. *Renewable Energy Review*, 22(4): 50–64.
- Bhutto, J. K. (2025). Coordinated hybrid VAR compensation using grid-forming battery energy storage systems for enhanced stability in inverter-dominated power systems. *Sustainability*, 17(23), 10820–10825.
- Buraimoh, A. and Davidson, IE. 2020. Power electronics interface for renewable energy integration: A review. *IEEE Access*, 8: 67620.
- Carrasco, J. M., Franquelo, L. G., Bialasiewicz, J. T. and Galván, E. 2013. Power-electronic systems for the grid integration of renewable energy sources: A survey. *IEEE Transactions on Industrial Electronics*, 53(4), 1002–1016.

Chen, Y., Liu, X., Zhang, H. and Wang, Z. 2025. Fault ride-through enhancement of photovoltaic systems using coordinated control of battery energy storage systems. *International Journal of Electrical Power & Energy Systems*, 154: 109432.

IEEE Standards Association. 2018. IEEE Standard for Interconnection and Interoperability of Distributed Energy Resources with Associated Electric Power Systems Interfaces (IEEE Std. 1547-2018).

Ding, G., Li, Y. and Zhang, X. 2016. Adaptive DC-link voltage control for photovoltaic inverters under grid faults. *IEEE Transactions on Industrial Electronics*, 63(3): 1568–1578.

Eskandari, M., Hasan, M. and Abed, N. 2022. Battery energy storage for fault ride-through enhancement in PV systems. *IEEE Access*, 10: 72345–72357.

Farhadi, M., Kangarlu, MF., Neyshabouri, Y. and Talavat, V. 2025. Low-voltage ride-through enhancement of a two-stage grid-connected photovoltaic system using battery energy storage and model predictive control. *International Journal of Renewable Energy Development*, 14(3): 404–419.

Giovanni, L., Marco, R. and Andrea, P. 2024. Grid support enhancement of photovoltaic systems through battery energy storage during voltage disturbances. *Electric Power Systems Research*, 227: 109879.

Güler, N., Demir, M. and Öztürk, S. 2025. Voltage stability enhancement of grid-connected renewable energy systems using battery energy storage systems. *IEEE Access*, 13: 45621–45633.

Kabir, E., Kumar, P. and Adelodun, B. 2018. Solar photovoltaic energy progress and future prospects. *Renewable and Sustainable Energy Reviews*, 82(1): 894–900.

Leibowicz, BD. 2015. Growth in global solar photovoltaic capacity and system reliability. *Energy Policy*, 87: 123–133.

Morey, M., Gupta, N., Garg, MM. and Kumar, A. 2023. A comprehensive review of grid-connected solar photovoltaic system: Architecture, control, and ancillary services. *Renewable Energy Focus*, 45: 307-330.

Obeidat, F. 2018. Renewable energy integration and grid fault management in solar PV systems. *Energy Reports*, 4: 512–521.

Obi, M. and Bass, R. 2016. Trends and challenges of grid-connected photovoltaic systems – A review. *Renewable and Sustainable Energy Reviews*, 58: 1082–1094.

Sadnan, M., Rahman, MM. and Islam, MS. 2025. Fault ride-through performance improvement of grid-connected photovoltaic systems using energy storage-based control strategies. *Energy Reports*, 11: 1523–1535.